Hindawi
Advances in Polymer Technology
Volume 2020, Article ID 5047487, 12 pages
https://doi.org/10.1155/2020/5047487

Research Article

A Novel Gel Polymer Electrolyte by Thiol-Ene Click Reaction Derived from CO_2-Based Polycarbonate for Lithium-Ion Batteries

Wenhan Luo,[1,2] Kuirong Deng,[1] Shuanjin Wang,[1] Shan Ren,[1] Dongmei Han,[3] Yufei Wang,[4] Min Xiao ,[1] and Yuezhong Meng [1]

[1]*The Key Laboratory of Low-carbon Chemistry & Energy Conservation of Guangdong Province/State Key Laboratory of Optoelectronic Materials and Technologies, School of Materials Science and Engineering, Sun Yat-sen University, Guangzhou 510275, China*
[2]*College of Light Industry and Food, Zhongkai University of Agriculture and Engineering, Guangzhou, China*
[3]*School of Chemical Engineering and Technology, Sun Yat-sen University, Zhuhai 519082, China*
[4]*Analytical and Testing Center of Guangzhou University, Guangzhou, China*

Correspondence should be addressed to Min Xiao; stsxm@mail.sysu.edu.cn and Yuezhong Meng; mengyzh@mail.sysu.edu.cn

Received 16 February 2020; Accepted 9 June 2020; Published 17 July 2020

Academic Editor: Yohei Kotsuchibashi

Here, we describe the synthesis of a CO_2-based polycarbonate with pendent alkene groups and its functionalization by grafting methoxypolyethylene glycol in view of its application possibility in gel polymer electrolyte lithium-ion batteries. The gel polymer electrolyte is prepared by an in-situ thiol-ene click reaction between polycarbonate with pendent alkene groups and thiolated methoxypolyethylene glycol in liquid lithium hexafluorophosphate electrolyte and exhibits conductivity as remarkably high as 2.0×10^{-2} S cm^{-1} at ambient temperature. To the best of our knowledge, this gel polymer electrolyte possesses the highest conductivity in all relevant literatures. A free-standing composite gel polymer electrolyte membrane is obtained by incorporating the gel polymer electrolyte with electrospun polyvinylidene fluoride as a skeleton. The as-prepared composite membrane is used to assemble a prototype lithium iron phosphate cell and evaluated accordingly. The battery delivers a good reversible charge-discharge capacity close to 140 mAh g^{-1} at 1 C rate and 25°C with only 0.022% per cycle decay after 200 cycles. This work provides an interesting molecular design for polycarbonate application in gel electrolyte lithium-ion batteries.

1. Introduction

Rechargeable lithium-ion batteries manifest enormous daily influence in electrochemical devices for microchip technology, consumer electronics, battery electric vehicles, and industrial energy storage [1, 2]. The electrolyte, providing the passage of ions to create the battery current, is a primary component of lithium-ion battery [3, 4]. Liquid electrolytes generally consist of lithium salts and organic solvent, including ethylene carbonate, propylene carbonate, dimethyl carbonate, or diethyl carbonate. These most conventional and typical volatile organic solvents sometimes produce volatilization and leakage issues during long-term operation [5–8]. Solid polymer electrolytes (SPE), defined as a polymer matrix dispersed with lithium salts, possess improved safety features, minimized dendrite growth, and good processability. However, the high interfacial impedance, low conductivity, and high cost on the contrary limit their areal application [9–13]. As a compromise proposal, gel polymer electrolytes (GPE) possess advantageous characteristics including high reliability, nonleakage, as well as high corresponding performance. Plentiful polymer matrixes, such as polyethylene oxide (PEO), [14–16] polyvinyl chloride (PVC), [17, 18] polyacrylonitrile (PAN), [19, 20] poly(methyl methacrylate) (PMMA), [21, 22] polyvinylidene fluoride (PVDF), [23–25] and poly (vinylidene fluoride-hexafluoropropylene) (PVDF-

HFP) copolymer, [26, 27], have been widely studied as frameworks in GPE. However, some handicaps, such as low ionic conductivity and transfer number, of GPE impede the performance of homologous batteries [28–30]. Various efforts have been devoted to design and modify polymer structure in order to improve battery performance [31–34].

Polycarbonates synthesized from CO_2 and epoxides have received considerable attention [35–37]. Conversion of CO_2 into economic, environment-friendly, and functional polycarbonates has been achieved since the pioneers Inoue and coworkers in 1969 [38]. Poly(propylene carbonate) (PPC), one of the most extensively studied CO_2-based polycarbonates, has also been studied as GPE due to the similar structure to conventional carbonate-based solvents applied in electrolytes. Yu and coworkers prepared PPCMA gel polymer electrolyte by the terpolymer of carbon dioxide, propylene oxide, and maleic anhydride. The ionic conductivity of the GPE at room temperature reaches up to 8.43×10^{-3} S cm^{-1} [39]. Zhao and coworkers explored a rigid-flexible coupling cellulose-supported PPC polymer electrolyte using $LiNi_{0.5}Mn_{1.5}O_4$ salt. The polymer electrolyte exhibited wider electrochemical window up to 5.0 V, higher ion transference number of 0.68, and higher ionic conductivity of 1.14×10^{-3} S cm^{-1} with commercial separator at room temperature [40]. Zhou and coworkers prepared a series of ionic liquid polymer electrolytes composed of PPC host, $LiClO_4$ and 1-butyl-3-methylimidazolium tetrafluoroborate ($BMIM^{+-}BF_4^-$), which exhibits a high ionic conductivity of 1.5×10^{-3} S cm^{-1} at room temperature [41]. Huang and coworkers developed poly(propylene carbonate)/poly(methyl methacrylate)-coated polyethylene gel polymer electrolyte, poly(vinylidene fluoride)/poly(propylene carbonate) gel polymer electrolyte, and polybutadiene rubber-interpenetrating cross-linking poly(propylene carbonate) network gel polymer electrolytes by physical blending methods and the corresponding coin cells achieve good charge-discharge capacity, cyclic stability, and rate performance [42–44]. In our previous work, CO_2-based and fluorinated polysulfonamide single-ion conducting CO_2-based polymer electrolytes for lithium-ion batteries has also been achieved, but the Li-ion conductivity was still low [45, 46].

No relevant research has ever reported GPE conductivity with the same order of magnitude compared to their liquid counterparts ($\sigma \approx 10^{-2}$ S cm^{-1}). In this work, we describe a novel GPE derived from functionalized CO_2-base polycarbonate to improve the lithium ionic conductivity and battery performance. This GPE was prepared from the terpolymer of propylene oxide (PO), allyl glycidyl ether (AGE), and CO_2. Functional thiolated polyethylene glycol (mPEG-SH) was grafted to the side chains through the thiol-ene click reaction. Compared to normal linear polycarbonate, the long, flexible branch group of PEG units benefits segmental mobility, which can improve the transport of lithium ions. The application feasibility in high-performance LIBs of this GPE is explored by electrochemical stability and ionic conductivity test. A skeleton of PVDF serves as a supporter and separator to manufacture composite membrane. The cell performance of the composite GPE was also evaluated.

2. Experimental

2.1. Materials. Propylene oxide (PO) and allyl glycidyl ether (AGE) were refluxed over CaH_2 for 20 hours and distilled under high pure nitrogen gas before use. Carbon dioxide of 99.99% purity was supplied from a high-pressure cylinder equipped with copper pipe and relief valves. Zinc glutarate (ZnGA) catalyst was prepared according to our previous work [47]. 3-Mercaptopropionic acid (MPA, 99%), methoxypolyethylene glycol (mPEG, average molecular 2000), 2,6-di-tert-butyl-4-methylphenol (BHT, 99.5%), p-toluenesulfonic acid (PTSA, 99%), and 2,2-dimethoxy-2-phenylacetophenone (DMPA, 99%) were purchased from Aladdin. $LiFePO_4$ (MTI Kejing Co., Ltd), Super P (TIMCAL), and poly(vinylidiene-fluoride) (PVDF, Arkema) were used as received without further purification. Solvents such as methanol, tetrahydrofuran, dichloromethane, hydrochloric acid, and diethyl ether were all analytical reagent grade and used without any further treatment.

2.2. Synthesis of PPCAGE. A 500 mL high-pressure autoclave equipped with a programmable temperature controller and a stainless-steel mechanical stirrer was used to carry out the terpolymerization of PO, AGE, and CO_2. Typically, 1.0 g ZnGA catalyst was placed into the autoclave. Then, the autoclave with the catalyst inside was sealed and further dried for 6 h under vacuum at 120°C. After cooling down to room temperature, PO and AGE with 8 : 2 molar ratio were inhaled into the vacuumed autoclave immediately. Then, the autoclave was pressurized to 5.0 MPa with CO_2 and maintained at 60°C. After 40 hours, the autoclave was cooled down and CO_2 pressure release following. The primeval polymer was dissolved in moderate dichloromethane and 0.5 g of BHT was appended into the solution to prevent the self-crosslinking phenomenon. The viscous solution polymer solution acid was poured into high-speed stirred cold ethanol detergent with 5% hydrochloric until all albus polymer was precipitated. The purification was repeated twice to completely remove catalyst and monomers. The ultimate polymer precipitates (PPCAGE) were dried under vacuum at 50°C for more than 24 h to pull out the solvent.

2.3. Thiolation of mPEG Using Mercaptoacetic Acid. A quantity of 12.0 g (6 mmol) mPEG and 6.36 g (60 mmol) MPA were dissolved in 100 mL toluene. The mixture was stirred and heated to 50°C. Then, 0.109 g (0.6 mmol) of PTSA was introduced into the solution. The thiolation reaction waged after the solution further heated to 130°C, stirred, and refluxed overnight in a dean-stark apparatus. A small quantity was analyzed by ^{1}H NMR to verify the complete reaction. The crude mixture was refined by precipitating in 2 L of ether. The mPEG-SH intermediate yield was 94% (11.86 g).

2.4. In-Situ Preparation of GPE@PVDF Membrane. Electrospun PVDF membrane was obtained according to Huang's work [34]. A typical 10% polymer content gel electrolyte precursor was prepared as follow: 0.202 g (0.33 mmol alkene) PPCAGE, 0.693 g (0.33 mmol) mPEG-SH, and 8.45 mg (0.033 mmol) of DMPA were dissolved in 8.05 g of 1 M $LiPF_6$/EC/DMC liquid electrolyte followed by stirring for 4 h till

all polymer dissolved. 20 μL precursor was added dropwise onto the PVDF membrane. After 5 min soak, the composite membrane was exposed to UV light (365 nm) for 10 min, then the membrane was ready to test and assemble cell.

2.5. Materials Characterization. ^{1}H NMR spectra of the polymers were recorded by Bruker DRX-500 NMR spectrometer, using chloroform-d ($CDCl_3$) as solvent and tetramethylsilane as internal standard. Polymer molecular weight (Mw and Mn) of resultant product was measured by gel permeation chromatography (GPC) system (Waters 515 HPLC Pump, Waters 2414 detector) with a set of columns (Waters Styragel 500, 10,000, and 100,000 Å) and chloroform (HPLC grade) as eluent. Glass transition temperature (T_g) of the samples was determined from the second heating run by a differential scanning calorimeter (DSC, Netzsch Model 204).

2.6. Ionic Conductivity Measurement. Ionic conductivities of the PPCAGE-g-mPEG GPEs were demonstrated by electrochemical impedance spectroscopy (EIS). The GPEs were in-situ prepared in an electrolytic tank in an argon atmosphere inside a glovebox. The equipment was placed into a self-designed vessel alongside a temperature controller. Electrochemical impedance spectroscopy in the 1 Hz to 1 MHz frequency range with an AC excitation voltage of 10 mV A was recorded by a Solartron 1255B frequency response analyzer in a temperature range of 25 to 80°C after maintaining the samples at each test temperature for over 1 h till thermal equilibration state. The bulk resistance can be calculated according to the equivalent fit circuit model to the data. The ionic conductivity (σ) was calculated by the equation as follow:

$$\sigma = \frac{L}{R_b A}, \tag{1}$$

where L is the thickness of the sample, R_b is the bulk resistance, and A is the effective overlap area of the sample.

2.7. Electrochemical Stability Window Measurement. The electrochemical stability window was determined by linear sweep voltammetry (LSV). GPE@PVDF membrane was stacked up with lithium foil as a reference electrode between stainless steel working electrodes. The tests were performed between 0 and 6.0 V (vs. Li/Li^+) at the scan rate of 1 mV s^{-1}.

2.8. Assemble LFP/GPE@PVDF/Li Coin Cell. With a weight ratio of 80 : 10 : 10, lithium iron phosphate (LFP), carbon black (CB), and PVDF were mixed up and grinded in NMP. The above mixture was then cast onto aluminum foil and dried at 80°C to prepare the cathode plate. The loading of LFP is around 1.7 mg cm^{-2}. The battery was assembled by sandwiched LFP plate, GPE@PVDF membranes (PVDF/liquid electrolyte membrane for comparison), and Li wafer seriatim. Then, the battery was sealed into a 2032 type coin cell by a tablet press. Charge and discharge tests for all batteries were performed at room temperature in a calorstat. The upper cut-off voltage was set at 4.0 V and the lower cut-off voltage at 2.5 V.

3. Results and Discussion

3.1. Terpolymerization of PO, AGE, and CO_2. Terpolymerization of PO, AGE, and CO_2 (Scheme 1 and Table S1) was successfully realized using ZnGA as an effective catalyst under 5.0 MPa CO_2 atmosphere at 60°C in a high-pressure autoclave.

The ^{1}H NMR spectrum of purified terpolymers (PPCAGE) is shown in Figure 1. The chemical shift at 5.1 −5.3 ppm and 5.8 ppm correspond to allyl groups –CH=CH_2 from allyl glycidyl ether monomer, showing that the AGE units were incorporated into the PPC mainchain successfully. The resonance peaks at 4.2 and 5.0 ppm are assigned to CH_2 and CH in the carbonate unit, respectively. The tiny peaks at 3.4–3.7 ppm corresponding to ether linkages indicate that the terpolymer is an alternating copolymer of epoxides and CO_2, consisting of PO-CO_2 carbonate units and AGE-CO_2 carbonate units. The mole percentage of the AGE-CO_2 carbonate unit is 12.2% according to the peak area of the peak at 5.8 ppm and 5.0 ppm. The resulting PO versus AGE ratio within the terpolymers is higher than the feed ratio, which illustrates that the polymerization reactivity of PO is higher than that of AGE.

A unimodal GPC trace of polymer product shown in Figure S1 indicates the molecular weight of 68400 and provides the direct evidence that the resulting polymer is a terpolymer rather than a mixture of PPC homopolymer and PAGEC homopolymer. Usually, the GPC trace of the mixture will more likely to be multiplet.

DSC measurement shows the amorphous character of the terpolymers, without any melting point (Figure S2). The glass transition temperature of the terpolymers is lower than 11.0°C. This is because that AGE units possess a flexible long pendant group, which favors segmental motion. The PPCAGE polymer is further functionalized to prepare new brand gel polymer electrolytes (GPEs). TGA curve of terpolymer PPCAGE also shows a decomposition temperature around 300°C (Figure S3).

3.2. Thiolation of Polyethylene Glycol Momomethyl Ether. Synthesis of thiol-functionalized mPEG-SH (Scheme 2) were achieved by esterification coupling between the hydroxyl end of mPEG and the carboxylic acid groups of MPA using PTSA as catalyst and toluene as solvent.

After precipitating the products in ether to remove MPA unit and PTSA catalyst, ^{1}H NMR spectra (Figure 2(a)) was used for product identification. The proton peaks at 1.6–1.7 ppm correspond to thiol proton. Peaks at 2.7–2.8 ppm correspond to the proton covalent in methylene next to thiol group. Peaks at 3.7 ppm correspond to PEG backbone. In particular, the peaks at 3.7 ppm and 4.3 ppm prove a successful couple between mPEG and MPA. FTIR spectroscopy further confirmed that thiol groups are present in the product (S-H stretch at 2550 cm^{-1}), as shown in Figure 2(b).

3.3. Grafting mPEG on PPCAGE via Thiol–Ene Click Reaction. Synthesis of PPCAGE-g-mPEG grafted polymer was successfully realized by a rapid thiol-ene click reaction with high reaction selectivity and conversion, quick reaction

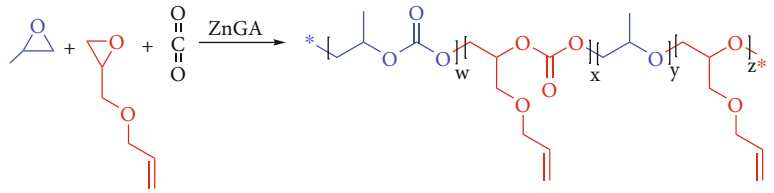

Scheme 1: Terpolymerization of propylene oxide (PO), allyl glycidyl ether (AGE), and carbon dioxide (CO_2) catalyzed by ZnGA.

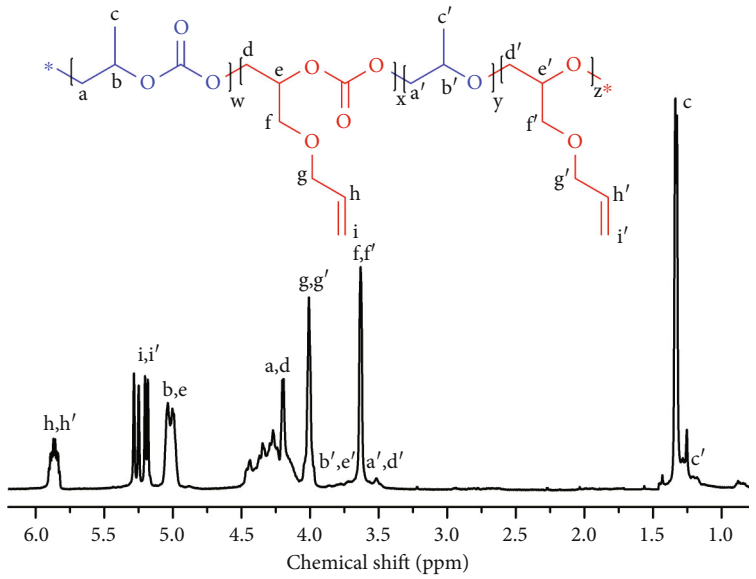

Figure 1: ^{1}H-NMR spectrum of terpolymer PPCAGE.

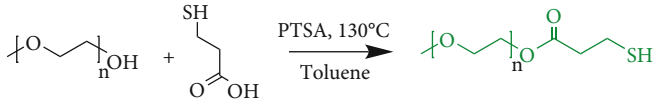

Scheme 2: Thiolation of polyethylene glycol momomethyl ethers with MPA.

rate, as well as moderate reaction conditions. Thiolated mPEG-SH can be easily grafted onto PPCAGE side chain via thiol-ene click reaction employing DMPA as photoinitiator in common 1 M $LiPF_6$/EC/DMC liquid electrolyte (Scheme 3).

The ^{1}H NMR spectrum of the resulting mPEG-grafted pendant polymer (PPCAGE-g-mPEG) is shown in Figure 3. The methylene proton signals of the pendant mPEG are distinctly visible at 2.6 ppm and 2.8 ppm, which evidence the objective functionalization reaction. Disappearance of peaks at 5.1 to 5.3 ppm and 5.8 ppm corresponding to the proton in allyl groups –CH=CH_2 confirms the complete conversion of the alkene groups. A photo was taken to show the polymer solution transform before and after UV-irradiation (inserted in Figure 3), showing the mixture changed from cloudy solution into uniform and transparent gel. Another proof is given by IR and TGA spectrum in Figures S4 and S5.

3.4. Ionic Conductivity of GPEs. Figure 4 and Table S2 demonstrate the correspondence of ionic conductivity (σ) with temperature and polymer content in GPE. The ion conductivity of $LiPF_6$ liquid electrolyte is 2.3×10^{-2} S cm^{-1} at 25°C. Apparently from the experiment result, the ionic conductivity of GPE decreases with PPCAGE-g-mPEG polymer content increasing. The value decreases to 2.0×10^{-2}, 1.7×10^{-2}, 1.5×10^{-2}, and 6.6×10^{-3} S cm^{-1} when polymer content is 5 wt.%, 10 wt.%, 20 wt.% and 30 wt.%, in turns. According to the ion conduction mechanism in a similar system [43, 48], lithium-ion can shuttle back and forth through the gel layer via both liquid state route and polymer state route. It is reasonable since the ion conductivity depends on the concentration of Li^+ and mobility of Li^+. The more the PPCAGE-g-mPEG solid content, the less the concentration and mobility of Li^+, thus the lower the ionic conductivity is. To better understand the ion conduction behavior in a polymer electrolyte, the activation energy Ea can be estimated by fitting the curves in Figure 4 to Arrhenius equation:

$$\sigma = \sigma_0 \exp\left(\frac{-E_a}{RT}\right), \quad (2)$$

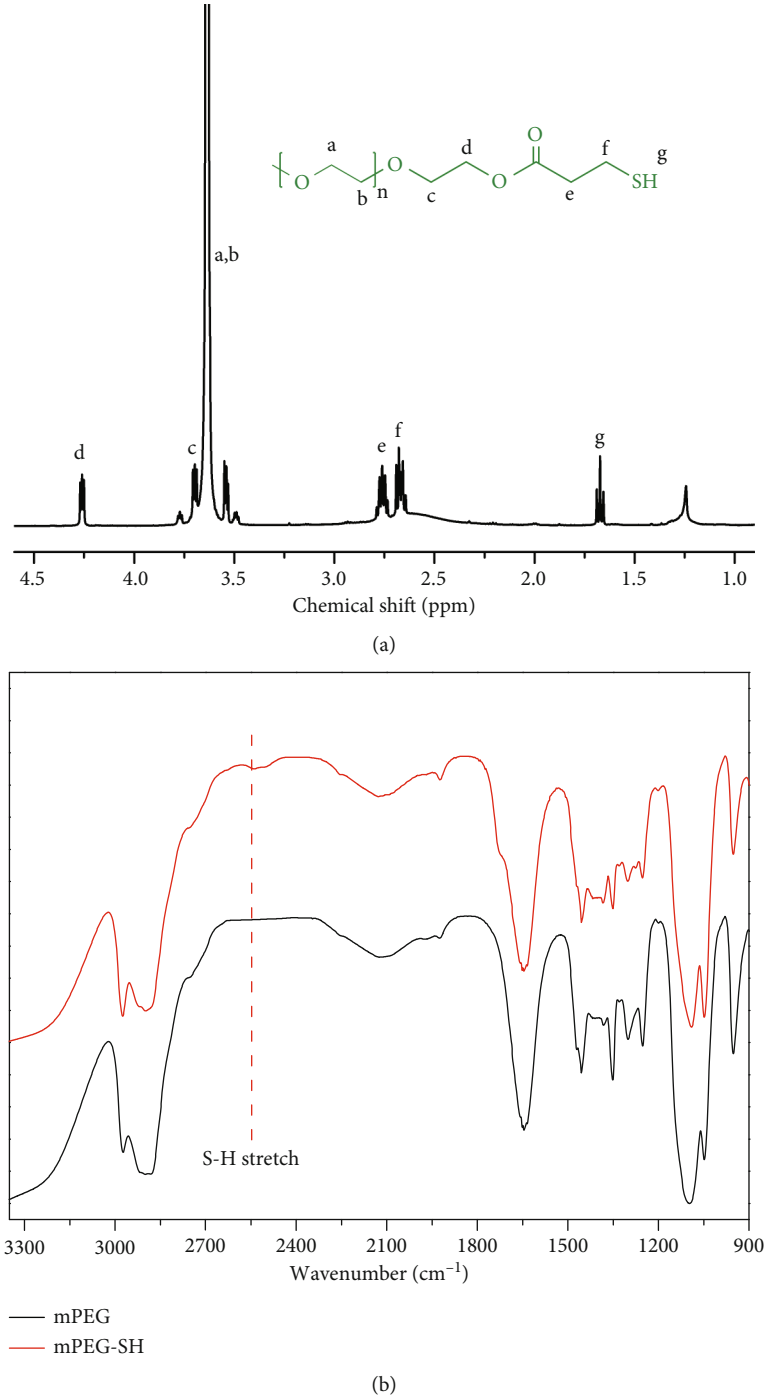

Figure 2: (a) ^{1}H-NMR spectrum of mPEG-SH; (b) IR spectrum of mPEG before and after thiolation.

Where σ is the ionic conductivity, σ_0 is a pre-exponential factor, R is the Boltzmann constant, and T is the temperature. E_a could be calculated from the slopes of the linear relationship. The E_a value of the GPE with 5 wt.%, 10 wt.%, 20 wt.%, and 30 wt.% polymer contents are in turns incremental 1.02, 1.21, 1.27, and 1.90 kJ mol^{-1}. On the base of free volume model, the activation energy depends on the mobility of ion carriers [49]. This is reasonable since the increase in PPCAGE-g-mPEG polymer matrix content can affect liquid electrolyte ratio, which involuntarily results in mobility descension of the carriers.

3.5. Fabrication of GPE@PVDF Membrane. Because of sticky nature and weak strength of PPCAGE-g-mPEG gel electrolyte, it is hard to scissors into a desire shape. An electrospun PVDF membrane was utilized to be the scaffold. In the line of the preparation method given in Section 2.4, the grafted polymer gel was incorporated into surface

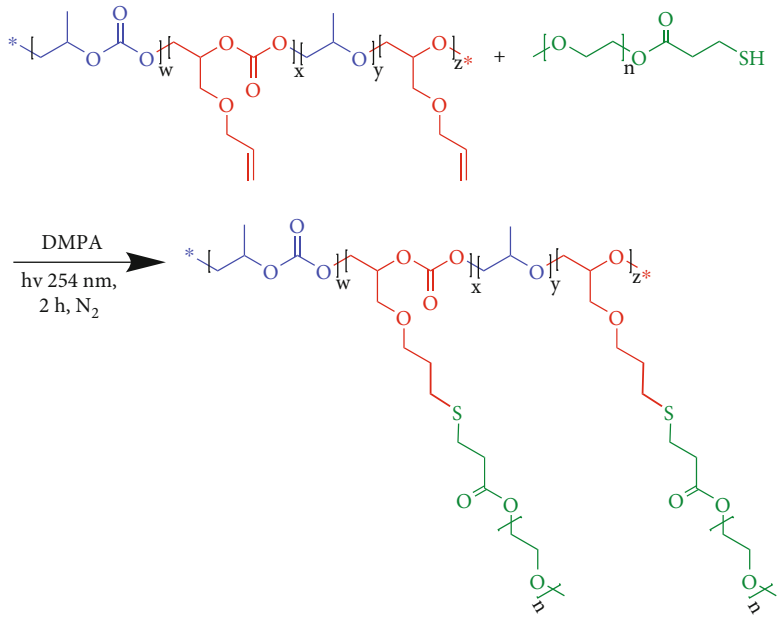

Scheme 3: Synthesis of PPCAGE-g-mPEG grafted polymer.

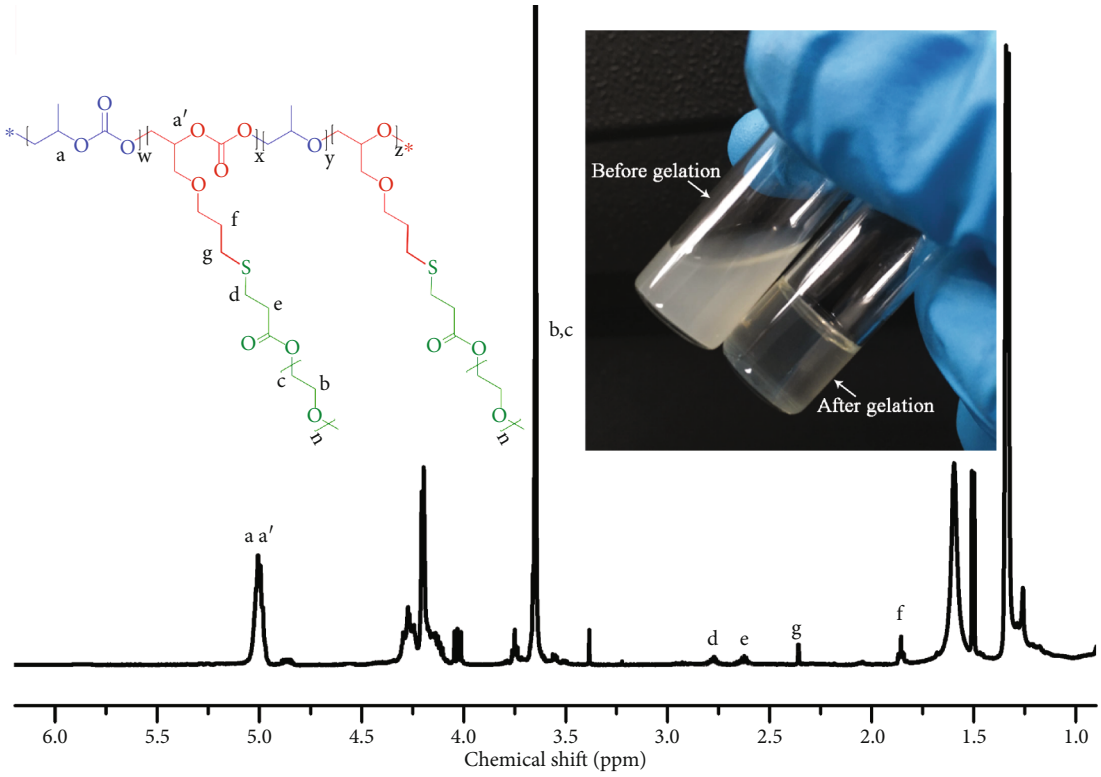

Figure 3: ^{1}H-NMR spectrum of PPCAGE-g-mPEG with inserting photo of the polymer solution before and after UV-irradiation.

and pores of PVDF separator to fabricate GPE@PVDF composite membrane. The morphologies of electrospun PVDF membrane and the composite gel electrolyte membrane are clearly observed from SEM images shown in Figure 5.

The primary PVDF separator has a visibly fibrous and porous structure. While PVDF skeleton is crop-full by PPCAGE-g-mPEG gel, the surface of PVDF separator is also soaked with gel mass. A notable feature is the transformation of PVDF surface morphology. With increasing polymer gel

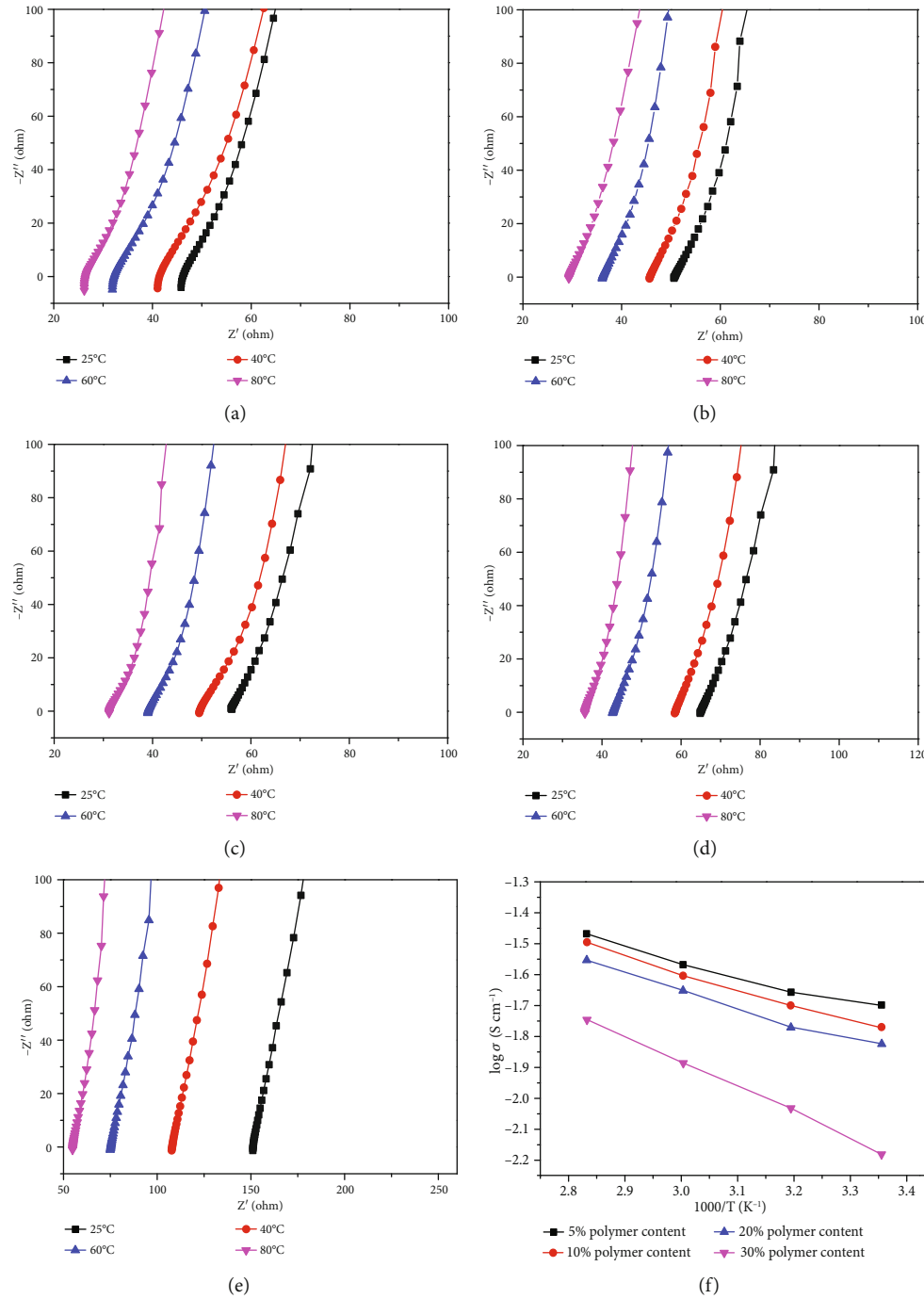

Figure 4: EIS plots for (a) liquid electrolyte and (b) 5% polymer content, (c) 10% polymer content, (d) 20% polymer content, (e)30% polymer content PPCAGE-g-PEG gel at different temperatures. (f) Temperature characteristic curves of ionic conductivity of PPCAGE-g-mPEGs with different polymer content.

concentration, the surface pore can be fully covered by a PPCAGE-g-mPEG gel layer. The white porous PVDF membrane becomes transparent as shown in Figure 5(d). Sulphur (root in original thiol group) distribution (Figure 5(c)) indicates a uniform distribution of PPCAGE-g-mPEG in composite membrane.

3.6. Electrochemical Stability of the GPE@PVDF Membrane. For commercial lithium ion battery, the potential can hit as high as 4.0 V vs. Li/Li^+. Therefore, the gel polymer electrolyte (GPE) needs be electrochemically stable at lease over 4.0 V. Figure 6 shows the linear sweep voltammetry curves of the cells employing GPE (10% polymer content) @ PVDF membrane as a separator. No rapid rise in current is detected till 4.5 V vs. Li/Li^+ for the GPE@PVDF membrane, indicating that the gel polymer electrolyte may be compatible with commercial lithium-ion battery. The conductivity of the GPE@PVDF membrane is

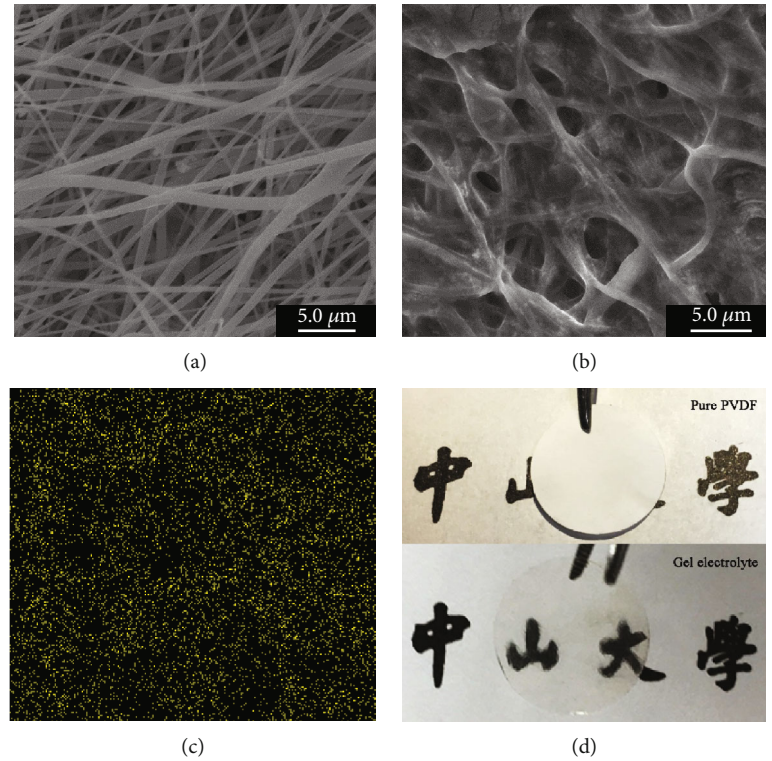

Figure 5: (a) SEM image of original PVDF separator, (b) SEM image of GPE@PVDF membrane, (c) Sulphur distribution in GPE@PVDF membrane, and (d) Photos of PVDF separator and GPE @ PVDF membrane.

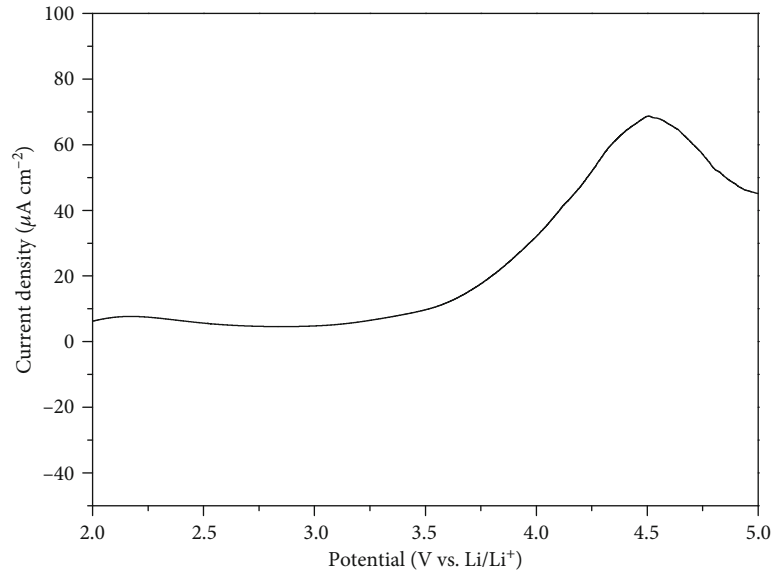

Figure 6: Linear sweep voltammogram of GPE@PVDF membrane.

calculated to 1.4×10^{-3} S cm^{-1} from Figure S6. Values of initial and steady-state currents (I_0, I_S), and interfacial resistances (R_0, R_S) of symmetric Li/Li$^+$ cells with the GPE@PVDF membrane were evaluated by polarization curves and impedance spectra as shown in Table S3 and Figure S7. It is believed that GPE@PVDF possesses better T_{Li+} (lithium transference numbers) compared to the pure PVDF membrane.

3.7. Battery Performances. The applicability of the GPE@PVDF membrane was further estimated by cell assembly with metallic lithium foil anode and LFP cathode.

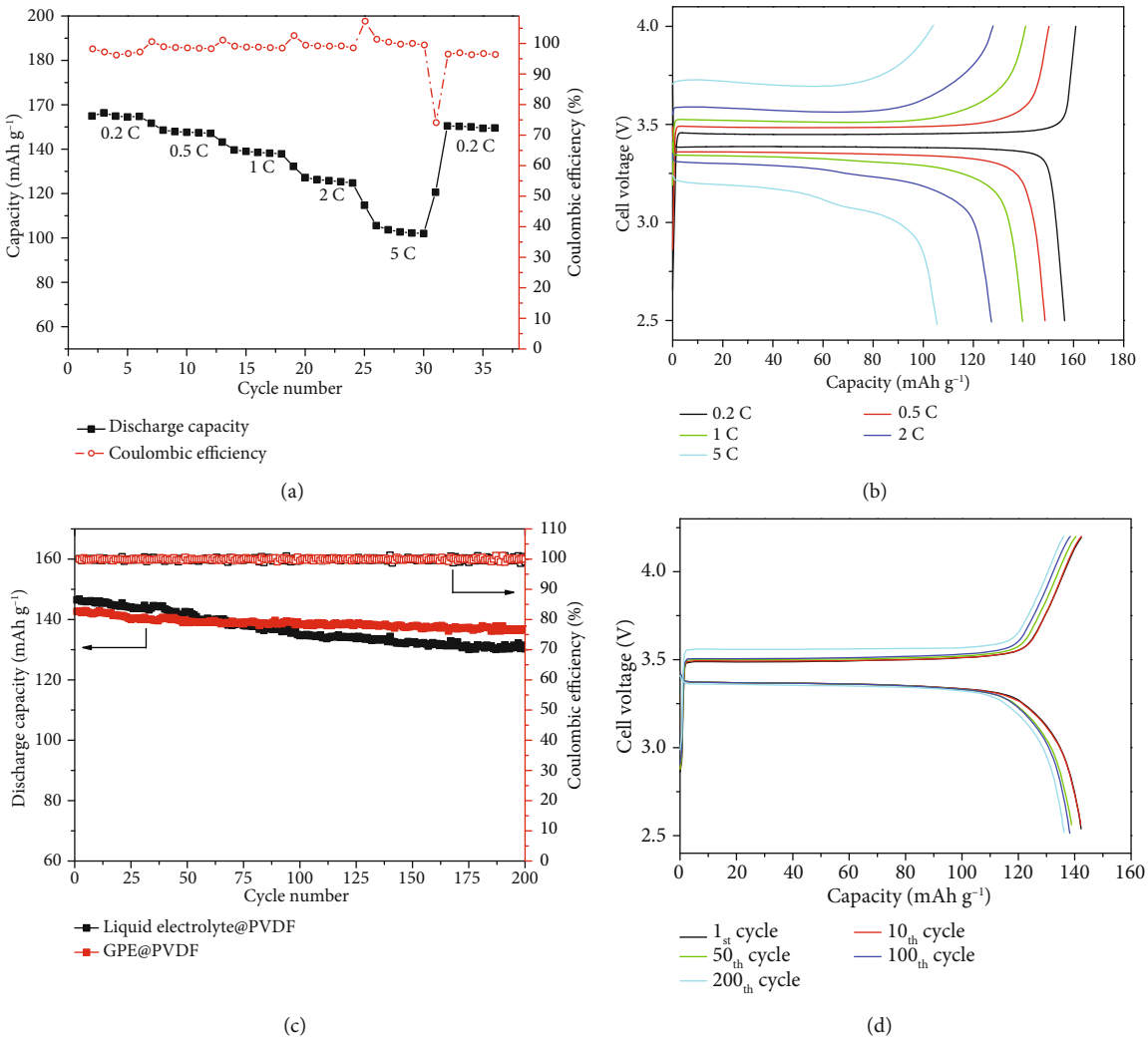

Figure 7: (a) Rate performance and (b) typical charge–discharge curves at various rates of GPE (10% polymer content) @ PVDF membrane cells; (c) cycling performance of liquid electrolyte @ PVDF cells and GPE (10% polymer content) @ PVDF membrane cells at 1 C; (d) typical charge–discharge curves of GPE (10% polymer content) @ PVDF membrane cells at 1 C.

Figure 7(a) shows the rate performances of the cells using GPE (10% polymer content) @ PVDF membrane at 25°C. Relatively stable capacities around average 163.4, 150.3, 141.6, 129.4, and 107.2 mAh g^{-1} are obtained at current rates of 0.2 C, 0.5 C, 1 C, 2 C, and 5 C, in their turns. The capacity at 5 C current rate retains 66% of original capacity at 0.2 C. As the current rate reverses back to 0.2 C, the initial capacity retains at 161.2 mAh g^{-1}, very close to initial capacity. Figure 7(b) shows the charge-discharge profiles of rate performance GPE@PVDF membrane cell. Flat voltage plateaus at around 3.5 V for battery charging and 3.4 V for battery discharging correspond to Fe^{3+}/-Fe^{2+} reversible redox couple reaction on the cathode [33]. At the initial charge or discharge stage, the terminal voltage of the battery rises or drops rapidly. The higher charge-discharge rate is, the faster battery voltage rises or drops. When the battery voltage enters a slowly changing platform area, the lower the charge or discharge rate is, the longer the platform area lasts and the slower the voltage rises or drops. These features are quite similar to liquid electrolyte batteries.

Figure 7(c) shows the cycling performances of liquid electrolyte @ PVDF cell and GPE (10% polymer content) @ PVDF membrane cell at 1 C at room temperature. Both of the two cells displayed good cycling performance with trifling capacity loss over 200 cycles at 1 C rate. The specific capacity of LFP cathode in GPE@PVDF membrane cell remained as high as 136.4 mAh g^{-1} after 200 cycles with a decay rate of only 0.022% per cycle. On the contrast, LFP cathode in liquid electrolyte @ PVDF cells is 130.4 mAh g^{-1} after 200 cycles with a decay rate of 0.055% per cycle. This result indicates that GPE @ PVDF membrane cell is more stable. One important reason for the decrease of battery stability is the lithium dendrite formed in the cathode. Polymer gel inhibits the generation of lithium dendrite and protects the cathode thus the stability of the battery is improved. On the other hand, a stable and uniform solid electrolyte interface (SEI) layer between polymer gel and the cathode can be formed in the charge and discharge processes. This passivation layer possesses the electronic-insulating characteristic similar to the

solid electrolyte as well as excellent lithium-ion conductivity. Lithium-ion can embed and strip freely though the passivation layer without making the cathode corrosion, so as to improve the stability of the battery.

Figure 7(d) shows the cycling performance of GPE@PVDF membrane cells. According to the low voltage polarization and stable cycle capacity, as both electrolyte and separator, the GPE@PVDF membrane provides good electrochemical performances for the cell operation. The competitive results for the electrolyte systems demonstrate that the PPCAGE-g-mPEG gel electrolyte has potential applications in lithium-ion batteries applying.

4. Conclusions

Terpolymer (PPCAGE) with alkene pendent can be readily synthesized by terpolymerization of PO, AGE, and CO_2 employing ZnGA as catalyst. This alkene pendent can be subsequently functionalized via rapid and efficient thiol-ene click reaction with mPEG-SH in liquid electrolyte, to afford a new kind of gel polymer electrolyte. The novel gel polymer electrolyte manifests the highest ionic conductivity as high as $2.0 \times 10^{-2}\,S\,cm^{-1}$ at 25°C. Meanwhile, LFP batteries with GPE@PVDF membrane as both separator and electrolyte show good rate performances and cycling performances. In conclusion, this work provides an alternative and efficient way to prepare a brand-new gel polymer electrolyte for lithium battery application utilizing environmentally friendly PEG grafted CO_2-based polycarbonate.

Data Availability

The authors confirm that the data supporting the findings of this study are available within the article and its supplementary materials.

Conflicts of Interest

The authors declare that they have no conflicts of interest.

Acknowledgments

The work was supported by the National Natural Science Foundation of China (U1601211, 51573215, 21506260, and 21706294), the Guangdong Province Sci & Tech Bureau (2017B090901003, 2016B010114004, and 2016A050503001), the Natural Science Foundation of Guangdong Province (2016A030313354), the Special Project on the Integration of Industry, Education and Research of Guangdong Province (2015B09090100), the Guangzhou Scientific and Technological Planning Project (201607010042, 201707010424, and 201804020025), the Fundamental Research Funds for the Central Universities (171gjc37), the University Research Project of Guangzhou 1201630241, and the Science and Technology Research Project of Guangzhou (Grant No. 201707010289).

Supplementary Materials

Figure S1: GPC curve of terpolymer PPCAGE with feed ratio of 80 : 20 (PO : AGE). Figure S2: DSC curve of terpolymer PPCAGE with feed ratio of 80 : 20 (PO : AGE). Figure S3: TGA curve of terpolymer PPCAGE with feed ratio of 80 : 20 (PO : AGE). Figure S4: IR spectrum of PPCAGE-g-mPEG showing a successful couple between PPCAGE and mPEG-SH. Figure S5: TGA curve of grafted polymer PPCAGE-g-mPEG. Figure S6: EIS plots for GPE @ PVDF membrane at room temperatures. The conductivity of the membrane is calculated to $1.4 \times 10^{-3}\,S\,cm^{-1}$. Figure S7: polarization curves and impedance spectra of (a) liquid electrolyte @ PVDF and (b) GPE@PVDF membrane with 10% polymer gel content. Table S1: results of the terpolymerization of CO2, PO, and AGE catalyzed by ZnGAa. Table S2: conductivity of PPCAGE-g-PEG gel electrolyte at different temperature. Table S3: values of initial and steady-state currents (I0, IS), and interfacial resistances (R0, RS) of symmetric Li/Li+ cells with the GPE @ PVDF membrane. *(Supplementary Materials)*

References

[1] L. Liu and C. Sun, "Flexible quasi-solid-state composite electrolyte membrane derived from a metal-organic framework for lithium-metal batteries," *ChemElectroChem*, vol. 7, no. 3, pp. 707–715, 2020.

[2] S. Li, X. Meng, Q. Yi et al., "Structural and electrochemical properties of $LiMn_{0.6}Fe_{0.4}PO_4$ as a cathode material for flexible lithium-ion batteries and self-charging power pack," *Nano Energy*, vol. 52, pp. 510–516, 2018.

[3] S. Huang, R. Guan, S. Wang et al., "Polymers for high performance Li-S batteries: material selection and structure design," *Progress in Polymer Science*, vol. 89, pp. 19–60, 2019.

[4] K. Xu, "Nonaqueous liquid electrolytes for lithium-based rechargeable batteries," *Chemical Reviews*, vol. 104, no. 10, pp. 4303–4418, 2004.

[5] A. Lewandowski and A. Świderska-Mocek, "Ionic liquids as electrolytes for Li-ion batteries—an overview of electrochemical studies," *Journal of Power Sources*, vol. 194, no. 2, pp. 601–609, 2009.

[6] D. Aurbach, Y. Ein-Ely, and A. Zaban, "The surface chemistry of lithium electrodes in alkyl carbonate solutions," *Journal of the Electrochemical Society*, vol. 141, no. 1, pp. L1–L3, 1994.

[7] M. Ishikawa, T. Sugimoto, M. Kikuta, E. Ishiko, and M. Kono, "Pure ionic liquid electrolytes compatible with a graphitized carbon negative electrode in rechargeable lithium-ion batteries," *Journal of Power Sources*, vol. 162, no. 1, pp. 658–662, 2006.

[8] P. G. Balakrishnan, R. Ramesh, and T. Prem Kumar, "Safety mechanisms in lithium-ion batteries," *Journal of Power Sources*, vol. 155, no. 2, pp. 401–414, 2006.

[9] J. W. Fergus, "Ceramic and polymeric solid electrolytes for lithium-ion batteries," *Journal of Power Sources*, vol. 195, no. 15, pp. 4554–4569, 2010.

[10] X. Li, J. Liu, M. N. Banis et al., "Atomic layer deposition of solid-state electrolyte coated cathode materials with superior high-voltage cycling behavior for lithium ion battery application," *Energy & Environmental Science*, vol. 7, no. 2, pp. 768–778, 2014.

[11] K. Yamamoto, Y. Iriyama, T. Asaka et al., "Direct observation of lithium-ion movement around an in-situ-formed-negative-electrode/solid-state-electrolyte interface during initial charge-discharge reaction," *Electrochemistry Communications*, vol. 20, pp. 113–116, 2012.

[12] Y. Li, W. Zhou, S. Xin et al., "Fluorine-doped antiperovskite electrolyte for all-solid-state lithium-ion batteries," *Angewandte Chemie International Edition*, vol. 55, no. 34, pp. 9965–9968, 2016.

[13] J. Li, C. Ma, M. Chi, C. Liang, and N. J. Dudney, "Solid electrolyte: the key for high-voltage lithium batteries," *Advanced Energy Materials*, vol. 5, no. 4, p. 1401408, 2015.

[14] Y. Kang, K. Cheong, K. A. Noh, C. Lee, and D. Y. Seung, "A study of cross-linked PEO gel polymer electrolytes using bisphenol A ethoxylate diacrylate: ionic conductivity and mechanical properties," *Journal of Power Sources*, vol. 119-121, pp. 432–437, 2003.

[15] H. Li, X. T. Ma, J. L. Shi, Z. K. Yao, B. K. Zhu, and L. P. Zhu, "Preparation and properties of poly (ethylene oxide) gel filled polypropylene separators and their corresponding gel polymer electrolytes for Li-ion batteries," *Electrochimica Acta*, vol. 56, no. 6, pp. 2641–2647, 2011.

[16] J. H. Shin, W. A. Henderson, and S. Passerini, "PEO-based polymer electrolytes with ionic liquids and their use in lithium metal-polymer electrolyte batteries," *Journal of the Electrochemical Society*, vol. 152, no. 5, pp. A978–A983, 2005.

[17] S. Rajendran, R. Babu, and P. Sivakumar, "Optimization of PVC- PAN-based polymer electrolytes," *Journal of Applied Polymer Science*, vol. 113, no. 3, pp. 1651–1656, 2009.

[18] P. Vickraman and S. Ramamurthy, "A study on the blending effect of PVDF in the ionic transport mechanism of plasticized PVC-$LiBF_4$ polymer electrolyte," *Materials Letters*, vol. 60, no. 28, pp. 3431–3436, 2006.

[19] S. W. Choi, J. R. Kim, S. M. Jo, W. S. Lee, and Y. R. Kim, "Electrochemical and spectroscopic properties of electrospun PAN-based fibrous polymer electrolytes," *Journal of the Electrochemical Society*, vol. 152, no. 5, pp. A989–A995, 2005.

[20] P. Carol, P. Ramakrishnan, B. John, and G. Cheruvally, "Preparation and characterization of electrospun poly (acrylonitrile) fibrous membrane based gel polymer electrolytes for lithium-ion batteries," *Journal of Power Sources*, vol. 196, no. 23, pp. 10156–10162, 2011.

[21] P. Meneghetti, S. Qutubuddin, and A. Webber, "Synthesis of polymer gel electrolyte with high molecular weight poly (methyl methacrylate)–clay nanocomposite," *Electrochimica Acta*, vol. 49, no. 27, pp. 4923–4931, 2004.

[22] S. Ramesh and G. P. Ang, "Impedance and FTIR studies on plasticized PMMA–$LiN(CF_3SO_2)_2$ nanocomposite polymer electrolytes," *Ionics*, vol. 16, no. 5, pp. 465–473, 2010.

[23] X. Wang, C. Gong, D. He et al., "Gelled microporous polymer electrolyte with low liquid leakage for lithium-ion batteries," *Journal of Membrane Science*, vol. 454, pp. 298–304, 2014.

[24] S. W. Choi, S. M. Jo, W. S. Lee, and Y. R. Kim, "An electrospun poly (vinylidene fluoride) nanofibrous membrane and its battery applications," *Advanced Materials*, vol. 15, no. 23, pp. 2027–2032, 2003.

[25] J. R. Kim, S. W. Choi, S. M. Jo, W. S. Lee, and B. C. Kim, "Electrospun PVDF-based fibrous polymer electrolytes for lithium ion polymer batteries," *Electrochimica Acta*, vol. 50, no. 1, pp. 69–75, 2004.

[26] Z. H. Li, C. Cheng, X. Y. Zhan, Y. P. Wu, and X. D. Zhou, "A foaming process to prepare porous polymer membrane for lithium ion batteries," *Electrochimica Acta*, vol. 54, no. 18, pp. 4403–4407, 2009.

[27] P. Yan, Z. Huang, Y. Lin et al., "Composite-porous polymer membrane with reduced crystalline for lithium–ion battery via non-solvent evaporate method," *Ionics*, vol. 21, no. 2, pp. 593–599, 2015.

[28] P. L. Kuo, C. A. Wu, C. Y. Lu, C. H. Tsao, C. H. Hsu, and S. S. Hou, "High performance of transferring lithium ion for polyacrylonitrile-interpenetrating crosslinked polyoxyethylene network as gel polymer electrolyte," *ACS Applied Materials & Interfaces*, vol. 6, no. 5, pp. 3156–3162, 2014.

[29] S. Li, D. Zhang, X. Meng, Q. A. Huang, C. Sun, and Z. L. Wang, "A flexible lithium-ion battery with quasi-solid gel electrolyte for storing pulsed energy generated by triboelectric nanogenerator," *Energy Storage Materials*, vol. 12, pp. 17–22, 2018.

[30] L. Long, S. Wang, M. Xiao, and Y. Meng, "Polymer electrolytes for lithium polymer batteries," *Journal of Materials Chemistry A*, vol. 4, no. 26, pp. 10038–10069, 2016.

[31] T. F. Miller III, Z. G. Wang, G. W. Coates, and N. P. Balsara, "Designing polymer electrolytes for safe and high capacity rechargeable lithium batteries," *Accounts of Chemical Research*, vol. 50, no. 3, pp. 590–593, 2017.

[32] G. Qiu and C. Sun, "A quasi-solid composite electrolyte with dual salts for dendrite-free lithium metal batteries," *New Journal of Chemistry*, vol. 44, no. 5, pp. 1817–1824, 2020.

[33] Q. Lu, J. Yang, W. Lu, J. Wang, and Y. Nuli, "Advanced semi-interpenetrating polymer network gel electrolyte for rechargeable lithium batteries," *Electrochimica Acta*, vol. 152, pp. 489–495, 2015.

[34] Y. Huang, B. Liu, H. Cao et al., "Novel gel polymer electrolyte based on matrix of PMMA modified with polyhedral oligomeric silsesquioxane," *Journal of Solid State Electrochemistry*, vol. 21, no. 8, pp. 2291–2299, 2017.

[35] D. J. Darensbourg, "Making plastics from carbon dioxide: salen metal complexes as catalysts for the production of polycarbonates from epoxides and CO_2," *Chemical Reviews*, vol. 107, no. 6, pp. 2388–2410, 2007.

[36] Q. Liu, L. Wu, R. Jackstell, and M. Beller, "Using carbon dioxide as a building block in organic synthesis," *Nature Communications*, vol. 6, no. 1, 2015.

[37] W. Luo, M. Xiao, S. Wang, D. Han, and Y. Meng, "Gradient terpolymers with long ε-caprolactone rich sequence derived from propylene oxide, CO_2, and ε-caprolactone catalyzed by zinc glutarate," *European Polymer Journal*, vol. 84, pp. 245–255, 2016.

[38] S. Inoue, H. Koinuma, and T. Tsuruta, "Copolymerization of carbon dioxide and epoxide with organometallic compounds," *Macromolecular Chemistry and Physics*, vol. 130, no. 1, pp. 210–220, 1969.

[39] X. Yu, M. Xiao, S. Wang, D. Han, and Y. Meng, "Fabrication and properties of crosslinked poly (propylene carbonate maleate) gel polymer electrolyte for lithium-ion battery," *Journal of Applied Polymer Science*, vol. 118, pp. 2078–2083, 2010.

[40] J. Zhao, J. Zhang, P. Hu et al., "A sustainable and rigid-flexible coupling cellulose-supported poly (propylene carbonate)

polymer electrolyte towards 5 V high voltage lithium batteries," *Electrochimica Acta*, vol. 188, pp. 23–30, 2016.

[41] D. Zhou, R. Zhou, C. Chen et al., "Non-volatile polymer electrolyte based on poly (propylene carbonate), ionic liquid, and lithium perchlorate for electrochromic devices," *The Journal of Physical Chemistry B*, vol. 117, no. 25, pp. 7783–7789, 2013.

[42] X. Huang, D. Xu, W. Chen et al., "Preparation, characterization and properties of poly (propylene carbonate)/poly (methyl methacrylate)-coated polyethylene gel polymer electrolyte for lithium-ion batteries," *Journal of Electroanalytical Chemistry*, vol. 804, pp. 133–139, 2017.

[43] X. Huang, S. Zeng, J. Liu et al., "High-performance electrospun poly (vinylidene fluoride)/poly (propylene carbonate) gel polymer electrolyte for lithium-ion batteries," *The Journal of Physical Chemistry C*, vol. 119, no. 50, pp. 27882–27891, 2015.

[44] X. Huang, J. Huang, J. Wu et al., "Fabrication and properties of polybutadiene rubber-interpenetrating cross-linking poly (propylene carbonate) network as gel polymer electrolytes for lithium-ion battery," *RSC Advances*, vol. 5, no. 65, pp. 52978–52984, 2015.

[45] K. Deng, S. Wang, S. Ren, D. Han, M. Xiao, and Y. Meng, "Network type sp3 boron-based single-ion conducting polymer electrolytes for lithium ion batteries," *Journal of Power Sources*, vol. 360, pp. 98–105, 2017.

[46] Y. Zhong, L. Zhong, S. Wang et al., "Ultrahigh Li-ion conductive single-ion polymer electrolyte containing fluorinated polysulfonamide for quasi-solid-state Li-ion batteries," *Journal of Materials Chemistry*, vol. 7, no. 42, pp. 24251–24261, 2019.

[47] Q. Zhu, Y.?. Z. Meng, S.?. C. Tjong, X.?. S. Zhao, and Y.?. L. Chen, "Thermally stable and high molecular weight poly (propylene carbonate)s from carbon dioxide and propylene oxide," *Polymer International*, vol. 51, no. 10, pp. 1079–1085, 2002.

[48] Y. Tominaga, K. Yamazaki, and V. Nanthana, "Effect of anions on lithium ion conduction in poly (ethylene carbonate)-based polymer electrolytes," *Journal of the Electrochemical Society*, vol. 162, no. 2, pp. A3133–A3136, 2015.

[49] Y. H. Li, X. L. Wu, J. H. Kim et al., "A novel polymer electrolyte with improved high-temperature-tolerance up to 170 ˚C for high-temperature lithium-ion batteries," *Journal of Power Sources*, vol. 244, pp. 234–239, 2013.